Real Time Evaluation of Binding Mechanisms in Multivalent Interactions: A Surface Plasmon Resonance Kinetic Approach

Eva Maria Munoz*, Juan Correa, Ricardo Riguera and Eduardo Fernandez-Megia*

Department of Organic Chemistry and Center for Research in Biological Chemistry and Molecular Materials (CIQUS), University of Santiago de Compostela, Jenaro de la Fuente s/n, 15782 Santiago de Compostela, Spain.

Supporting Information Placeholder

ABSTRACT. Multivalency is a key, ubiquitous phenomenon in nature characterized by a complex combination of binding mechanisms, with special relevance in carbohydrate–lectin recognition. Herein we introduce an original surface plasmon resonance (SPR) kinetic approach to analyze multivalent interactions that has been validated with dendrimers as monodisperse multivalent analytes binding to lectin clusters. The method, based on the analysis of early association and late dissociation phases of the sensorgrams provides robust information of the glycoconjugate binding efficiency and real-time structural data of the binding events under the complex scenario of the glycocluster effect. Notably, it reveals the dynamic nature of the interaction and offers experimental evidence on the contribution of binding mechanisms.

Multivalent interactions play a fundamental role in a plethora of physiological and pathological processes. The multivalent presentation of ligands and receptors results in higher relative binding affinities and specificities than monovalent interactions.[1,2,3] This strategy encountered by nature to modulate biorecognition events has also served as source of inspiration for the design of multivalent synthetic conjugates with therapeutic properties.[3,4] Carbohydrate–protein (lectin) recognition is by far the most studied multivalent interaction because of its relevance in key processes such as, cell–cell recognition, fertilization, pathogen invasion, and toxin and hormone mediation.[5] In this context, a vast number of multivalent synthetic glycoconjugates has been prepared over the last decades including dendritic scaffolds, linear polymers, micelles, nanoparticles, and nanotubes.[6,7,8] In contrast to the progress achieved in the competent synthesis of these conjugates, the precise evaluation of their binding properties is still limited by the complexity of the binding mechanisms associated to multivalent interactions. While the enhanced binding affinity through the so called glyco-cluster effect has been attributed to a combination of binding mechanisms (intermolecular cross-linking, chelation, and statistical rebinding or bind and slide mechanism),[7,8,9] no experimental procedures have been described so far to deconvolute their contributions to the overall binding.[7] As a consequence, binding data is frequently extracted from indirect competitive methods where only relative affinities are obtained.[10]

Aware of these limitations, we have recently reported a series of model surface plasmon resonance (SPR) binding experiments between mannosylated GATG (gallic acid-triethylene glycol) dendrimers and the lectin Concavalin A (ConA) that reveal the importance of performing direct, real time analysis of multivalent interactions.[11]. A complex binding profile was disclosed and two limiting binding modes were described: a low affinity binding mode associated to dendrimers binding a ConA surface monovalently, and a high affinity mode associated to dendrimers with higher functional valency. These results, together with theoretical investigations,[12,13] point to multivalent carbohydrate–lectin interactions as driven by a dynamic binding heterogeneity where the contribution of the different mechanisms depends not only on the glycoconjugate multivalency and lectin cluster density, but also on the local concentration of glycoconjugates in the proximity of the lectin cluster, which is a time-dependent factor. Accordingly, only by paying greater attention to the kinetic aspects of these interactions, a deeper understanding of the glycocluster effect would be achieved. Herein, we report an original SPR-based protocol designed to gather rich kinetic information on the interaction between multivalent analytes (glycoconjugates) and clustered receptors on a surface (lectins). The major pillar of the method consists in the real time monitoring and analysis of the interaction at low analyte local concentration nearby the receptor surface (early association and late dissociation phases of the sensorgrams), an experimental environment where the binding modes of higher affinity prevail. Application of this protocol is presented to the analysis of the interaction between GATG glycodendrimers[14,15] decorated with α-D-mannose and α-D-glucose ([Gn]-Man and [Gn]-Glc; being n the dendrimer generation) and ConA immobilized to sensor-chips as a model system for a clustered arrangement of lectins (Figure 1).
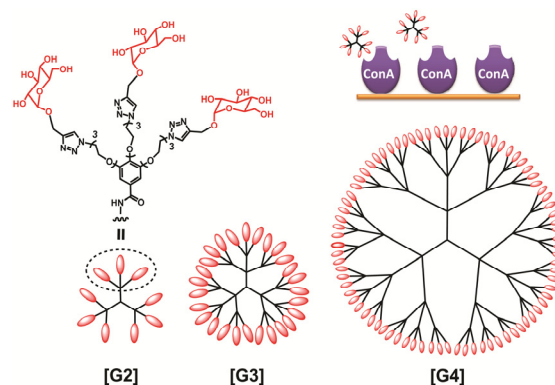

Figure 1. Schematic representation of the model multivalent system selected for this study: GATG glycodendrimers containing α-D-mannose or α-D-glucose and ConA clustered on SPR sensor chips.
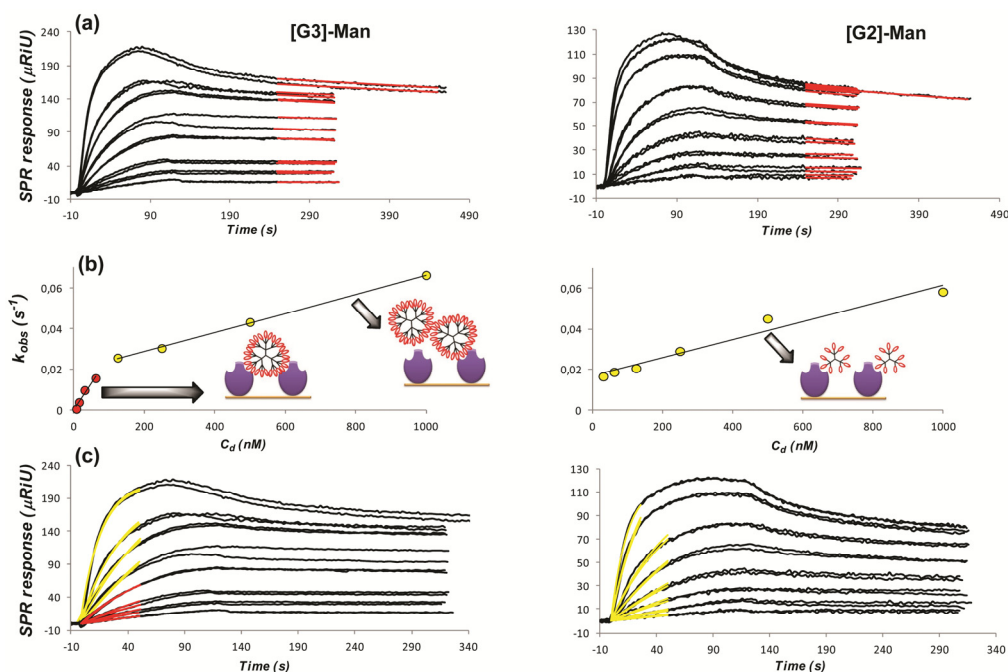
Figure 2. SPR separate kinetic analysis of the interaction of [G3]-Man and [G2]-Man (1000-7.8 nM) with ConA-HD. Step I (late dissociation phase kinetic analysis): (a) Sensorgrams (black) and global fitting (red) to pseudo-first order kinetics. Step II (early association phase kinetic analysis): (b) Plots of k_{obs} vs dendrimer concentration (C_d); and (c) sensorgrams (black) and global fitting of the early association phase (yellow and red) to the integrated rate equation for pseudo-first order kinetics.

To this end, ConA was covalently attached to a polycarboxylated SPR sensor chip to generate a high-density lectin surface (ConA-HD, with a SPR response of the immobilization of 10000 μRiU, 1 μRiU ~ 1 pg/mm^2). A titration with methyl-α-D-mannopyranoside (Me-Man) was first carried out to determine the binding activity of the surface by means of the maximum Me-Man binding capacity, which resulted in a SPR response of 20 μRiU (Figure S1a in the Supporting Information). Then, SPR titrations with [G2]-Man, [G3]-Man, and [G4]-Man (containing 9, 27, and 81 mannose residues) were performed towards ConA-HD by sequentially injecting increasing concentrations of the dendrimers (C_d) over the lectin surface (Figures 2 and S3). These experiments were conducted at low C_d (below 1 μM) to attain the circumstance of low local concentration that minimizes competition between glycodendrimers for binding to ConA. Binding tests at different flow rates were performed prior to the titrations to confirm the absence of mass transport effects influencing the shape of the sensorgrams (Figure S2).[16] As expected, the registered sensorgrams showed complex binding profiles consistent with the multivalent nature of the glycodendrimer–ConA interaction that failed to globally fit to conventional binding models.[11] Instead, a detailed kinetic analysis of the sensorgrams was carried out at the early association and late dissociation phases of the sensorgrams (Figure 2).

The first step of the method is the evaluation of the dissociation phase, shown in Figures 2a ([G2]-Man and [G3]-Man) and S3a ([G4]-Man). While a high degree of binding heterogeneity was found at early dissociation times (t = 120-245 s), late dissociation data (t ≥ 245 s) showed good fitting to the classical equation for pseudo first order kinetics:

$$R_t = R_0 \exp(-k_{off\text{-}high} (t-t_0)) \qquad (1)$$

where R_t is the SPR response at time t, R_0 is the response at the beginning of late dissociation (t_0 = 245 s), and $k_{off\text{-}high}$ is the apparent dissociation rate constant that accounts for the release of glycodendrimers

from the ConA surface stabilized by a multivalent effect. For [Gn]-Man, $k_{off\text{-}high}$ values were found to be four orders of magnitude lower than the calculated dissociation rate constant for the monovalent ConA–Me-Man complex ($k_{off\text{-}mono} \sim 6$ s^{-1})[17] (Table 1). Coherent differences in $k_{off\text{-}high}$ resulted when comparing different dendrimer generations, with [G4]-Man showing 2.2- and 3.9-fold slower dissociation than [G3]-Man and [G2]-Man. The same trend was observed when comparing the rate of dissociation at early dissociation times, provided as the percentage of SPR signal decay from 120 s to 245 s (for [G4]-Man was 1.6- and 2.8-fold times lower than [G3]-Man and [G2]-Man, Table S1). Overall, the remarkable slow dissociation of the glycodendrimers from the ConA-HD surface represents the main contribution to their enhanced binding affinity compared to the monosaccharide, and serves as a valuable analytical tool for comparing binding efficiencies. To complement this information with structural data, we moved to the second step of this method: a kinetic evaluation of the association phase of the sensorgrams.

The evaluation of early association (t ≤ 50 s) was initially performed by linear analysis of the equations described for pseudo first-order kinetics (Figures 2b and S3b):

$$dR/dt = k_{on} C_d R_{max} - k_{obs} R \qquad (2)$$

$$k_{obs} = k_{on} C_d + k_{off\text{-}high} \qquad (3)$$

where R_{max} is the SPR response matching to the maximum analyte binding capacity of the surface, and k_{on} and k_{obs} are association and observable rate constants, respectively. Since plotting of k_{obs} vs C_d gives a straight line with slope equal to k_{on} (see eq 3), binding heterogeneity might be explored based on deviations from this linear behavior.[18] The binding of [G3]-Man and [G4]-Man with ConA-HD yielded plots of k_{obs} vs C_d with two well defined slopes (Figures 2b and S3b). In both examples, the largest slope (faster association) was observed at low C_d. Knowing that multivalency typically increases the kinetic activity of interactions,[13] this result points towards the presence of higher order

Table 1. Binding data from separate kinetic analysis of [Gn]-Man and [Gn]-Glc dendrimers binding to ConA surfaces of high (HD) and low density (LD): k_{on} ($10^4 M^{-1}s^{-1}$), $k_{off-high}$ ($10^{-4} s^{-1}$), K_D (nM).

	ConA-HD			ConA-LD		
	k_{on-1}	k_{on-2}	$k_{off-high}$ ($K_{D,high}$)	k_{on-1}	k_{on-2}	$k_{off-high}$ ($K_{D,high}$)
[G2]-Man	7.1 ± 0.2		7.0 ± 0.01 (9.9)			
[G3]-Man	23.2 ± 0.1	5.8 ± 0.1	3.9 ± 0.1 (1.7)	8.5 ± 0.1		11.7 ± 0.2 (13.8)
[G4]-Man	44.1 ± 0.9	12.8 ± 0.1	1.8 ± 0.02 (0.4)	24.0 ± 0.5	14.7 ± 0.9	5.0 ± 0.1 (2.1)
[G2]-Glc	15.0 ± 0.4		18.3 ± 0.3 (12.2)			
[G3]-Glc	27.7 ± 0.6	9.2 ± 0.3	10.5 ± 0.1 (3.8)	11.7 ± 0.4		18.5 ± 0.5 (15.8)
[G4]-Glc	29.1 ± 1.3	6.7 ± 0.1	4.4 ± 0.1 (1.5)	38.5 ± 1.9	6.8 ± 0.3	8.2 ± 0.2 (2.8)

complexes in the low C_d range. Oppositely, for [G2]-Man, a single slope was displayed of magnitude comparable to those for [G3]-Man and [G4]-Man at high C_d (Figure 2b). As only estimates of k_{on} could be provided by the above linearization method, more precise values were pursued by global fitting the early association phase of the sensorgrams to the integrated rate equation for pseudo first-order kinetics (Figures 2c and S3c):

$$R_t = R_{eq} (1-exp(-(k_{on} C_d + k_{off-high}) t)) \qquad (4)$$

Global fitting of early association for [G3]-Man sensorgrams at $C_d >$ 62.5 nM yielded a k_{on-2} value typical of a monovalent Me-Man–ConA interaction ($k_{on-mono} \sim 5 \cdot 10^4 M^{-1}s^{-1}$),[17] while fitting at $C_d \le$ 62.5 nM afforded a k_{on-1} value ~ 4 times higher than that (Table 1). Noteworthy, it has been stated that binding of a divalent analyte with a divalent ligand occurs more readily by a factor of 4 compared to its monomeric counterpart.[12,13] This result suggests [G3]-Man is able to simultaneously bind two ConA sites on the ConA-HD surface. A similar behavior was exhibited by [G4]-Man although with k_{on-1} and k_{on-2} values exceeding those of [G3]-Man. A possible explanation to this observation is that [G4]-Man, with 3-fold more Man per dendrimer, benefits from a stronger rebinding effect that contributes to a subtle increase of the association rate. Finally, the fitting of [G2]-Man sensorgrams yielded a single k_{on} comparable to $k_{on-mono}$, which implies this dendrimer as not able to span two ConA sites in ConA-HD. Notably, this proposed early association phase analysis provides novel real-time structural information of the glycodendrimer–lectin cluster interaction and confirms that the contribution of binding mechanisms is a dynamic parameter that varies with the local concentration of glycoconjugates nearby the lectin surface, as schematically depicted in Figure S7. Thus, this method determines the ability of the glycoconjugate to span two sites of the lectin cluster and so, it identifies the stabilization mechanisms of the high affinity binding modes (chelation+ rebinding for [G3]-Man and [G4]-Man, rebinding for [G2]-Man). Last but not least, from the early association and late dissociation kinetic data shown in Table 1, estimates of the dissociation constants for the high affinity binding modes ($K_{D,high}$) can be extracted. This results in affinities higher than 2 nM for [G3]-Man and [G4]-Man which agree with the proposed chelation mechanism $[K_N^{poly} < (K^{mono})^N = (83 \mu M)^2 = 6.9 nM]$.[1] Importantly, [G2]-Man, unable to span two ConA sites on ConA-HD, displays a $K_{D,high}$ of only 9.9 nM, demonstrating the relevance of rebinding as stabilization mechanism under conditions of low local concentration.

To further validate this kinetic analysis, we decided to explore the GATG glycodendrimer–ConA interaction under two additional scenarios, which involved modification of intrinsic binding properties of the ConA cluster or the glycodendrimer. In the search of differences in the binding mode of the largest dendrimers, the interaction of [G4]-

Man and [G3]-Man was studied towards a second ConA surface with a functional lectin coverage half of that achieved in ConA-HD (ConA-LD, with a SPR response of the immobilization of 7500 μRiU and a maximum Me-Man binding capacity of 10 μRiU, Figure S1b). According to the dissociation phase analysis, the binding efficiency of both glycodendrimers decreased by 3-fold in ConA-LD as a result of the lower lectin density. The relative efficiency between generations is maintained, with $k_{off-high}$ for [G4]-Man being again 2.3-fold lower than [G3]-Man, and the signal decay at early dissociation 1.6 times lower for [G4]-Man than for [G3]-Man (Figure S4 and Tables 1 and S1). On the basis of the early association rate constant analysis, the high affinity binding mode for [G4]-Man still corresponds to a chelate while [G3]-Man benefits only from rebinding as source of stabilization in ConA-LD. The decrease in lectin density impedes [G3]-Man to simultaneously bind two ConA sites (Figure S4). Overall, lowering the lectin density results in reduced affinities and altered high affinity binding modes, as a response to variations in the relative size between the glycodendrimer and the interlectin distance.

In a second case study, the intrinsic binding properties of the glycodendrimers were modified by decoration with α-D-glucose (Glc) instead of α-D-mannose. The selection of Glc was done because it presents well-defined kinetic differences compared to Man. While both monosaccharides bind ConA with analogous $k_{on-mono}$ but the Glc–ConA complex dissociates ~ 4 times faster than Man–ConA.[19,20] First, a SPR titration of methyl-α-D-glucopyranoside (Me-Glc) vs ConA-HD was performed to confirm that glucose binds ConA with four times lower affinity than mannose (Figure S1c). [G2]-Glc, [G3]-Glc, and [G4]-Glc were then prepared (see details in the SI) and their binding efficiency was evaluated towards ConA-HD and ConA-LD following the above protocol (Figures S5 and S6). As expected, [Gn]-Glc dendrimers dissociate faster from the ConA surfaces as compared with [Gn]-Man. Notably, the relative dissociation rate among [Gn]-Glc series towards ConA-HD was analogous to that found for [Gn]-Man: i) $k_{off-high}$ of [G4]-Glc is 2.4 and 4.2 times lower than [G3]-Man and [G2]-Man, and ii) the signal decay at early dissociation times for [G4]-Glc is 1.8 and 2.6 times lower than [G3]-Glc and [G2]-Glc, respectively (Table S1). Similar information was extracted from the late dissociation phase analysis of [Gn]-Glc towards ConA-LD. These results can be interpreted as a proof of the usefulness of dissociation rate data to estimate the relative binding efficiency of multivalent scaffolds, independently on the nature of the carbohydrate. It was interesting to see that [Gn]-Glc dissociates only 2.6-fold faster than [Gn]-Man from ConA-HD, while a variation of at least 4-fold would be expected according to differences in the dissociation rate of mannose vs glucose.[20] A reasonable explanation to this behavior is that the intrinsic faster

dissociation of glucose results in a decreased number of dendrimers nearby the surface and a concomitant increased number of uncomplexed ConA sites, which facilitate an enhanced stabilization of [Gn]-Glc by rebinding.[21] In agreement with this scenario, an even more pronounced effect was observed when analyzing [Gn]-Glc–ConA-LD, which late dissociation rate differs only 1.6-fold from [Gn]-Man. This interesting effect stresses the dynamic nature of multivalent interactions at surfaces and reveals the concentration of glycoconjugate in the proximities of the lectin cluster as a relevant factor to consider, together with the lectin density or the size of the glycoconjugate, when determining the binding efficiency of these interacting systems. Finally, the analysis of the early association phase of the sensorgrams of [Gn]-Glc demonstrated again the robustness and fidelity of the method by affording: i) biphasic representations for [G4]-Glc and [G3]-Glc binding to ConA-HD, and [G4]-Glc to ConA-LD, and ii) k_{on} values in the range of [Gn]-Man (Figures S5b and S6b).

This study constitutes the first example of a detailed evaluation of multivalent carbohydrate–lectin interactions based on a SPR kinetic analysis of the early association and late dissociation phases of the sensorgrams. This protocol provides robust information of the glycoconjugate binding efficiency, rich real-time structural data, and experimental evidence on the dynamic contribution of chelate and rebinding mechanisms under the complex scenario of the glycocluster effect. We believe the information extracted from this analysis will conduct to a more successful evaluation and selection of optimal glycoconjugate architectures for particular purposes.

ASSOCIATED CONTENT

Supporting Information. Materials, synthesis and characterization of [Gn]-Glc glycodendrimers, SPR binding assays and separate kinetic analysis method. This material is available free of charge via the Internet at http://pubs.acs.org.

AUTHOR INFORMATION

evamaria.munoz@usc.es; ef.megia@usc.es

ACKNOWLEDGMENT

REFERENCES

(1) Mammen, M.; Choi, S.-K.; Whitesides, G. M. *Angew. Chem. Int. Ed. Engl.* **1998**, *37*, 2754.

(2) (a) Gestwicki, J. E.; Kiessling, L. L. *Nature* **2002**, *415*, 81. (b) Badjic, J. D.; Nelson, A.; Cantrill, S. J.; Turnbull, W. B.; Stoddart, J. F. *Acc. Chem. Res.* **2005**, *38*, 723. (c) Huskens, J. *Curr. Opin. Chem. Biol.* **2006**, *10*, 537.

(3) Fasting, C.; Schalley, C. A.; Weber, M.; Seitz, O.; Hecht, S.; Koksch, B.; Dernedde, J.; Graf, C.; Knapp, E. W.; Haag, R. *Angew. Chem. Int. Ed. Engl.* **2012**, *51*, 10472.

(4) (a) Markin, C. J.; Xiao, W.; Spyracopoulos, L. *J. Am. Chem. Soc.* **2010**, *132*, 11247. (b) Roglin, L.; Lempens, E. H.; Meijer, E. W. *Angew. Chem. Int. Ed.*

Engl. **2011**, *50*, 102. (c) Bernardi, A. et al. *Chem. Soc. Rev.* **2013**, doi 10.1039/C2CS35408J.

(5) Lundquist, J. J.; Toone, E. J. *Chem. Rev.* **2002**, *102*, 555.

(6) (a) Roy, R. *Curr. Opin. Struct. Biol.* **1996**, *6*, 692. (b) Chabre, Y. M.; Roy, R. *Adv. Carbohydr. Chem. Biochem.* **2010**, *63*, 165. (c) Becer, C. R.; Gibson, M. I.; Geng, J.; Ilyas, R.; Wallis, R.; Mitchell, D. A.; Haddleton, D. M. *J. Am. Chem. Soc.* **2010**, *132*, 15130. (d) Suriano, F.; Pratt, R.; Tan, J. P.; Wiradharma, N.; Nelson, A.; Yang, Y. Y.; Dubois, P.; Hedrick, J. L. *Biomaterials* **2010**, *31*, 2637. (e) Gorityala, B. K.; Ma, J.; Wang, X.; Chen, P.; Liu, X. W. *Chem. Soc. Rev.* **2010**, *39*, 2925. (f) Ribeiro-Viana, R.; Sanchez-Navarro, M.; Luczkowiak, J.; Koeppe, J. R.; Delgado, R.; Rojo, J.; Davis, B. G. *Nat. Commun.* **2012**, *3*, 1303. (g) Marradi, M.; Chiodo, F.; Garcia, I.; Penades, S. *Chem. Soc. Rev.* **2013**, doi 10.1039/C2CS35420A. (h) Peri, F. *Chem. Soc. Rev.* **2013**, doi 10.1039/C2CS35422E.

(7) Jayaraman, N. *Chem. Soc. Rev.* **2009**, *38*, 3463.

(8) Pieters, R. J. *Org. Biomol. Chem.* **2009**, *7*, 2013.

(9) (a) Mulder, A.; Huskens, J.; Reinhoudt, D. N. *Org. Biomol. Chem.* **2004**, *2*, 3409. (b) Kiessling, L. L.; Young, T.; Gruber, T. D.; Mortell, K. H. In Glycoscience; Fraser-Reid, Tatsuta and Thiem, Eds.; Springer: 2008, p 2483. (c) Dam, T. K.; Brewer, C. F. *Biochemistry* **2008**, *47*, 8470.

(10) For recent examples see: (a) Schlick, K. H.; Cloninger, M. J. *Tetrahedron* **2010**, *66*, 5305. (b) Schwefel, D.; Maierhofer, C.; Beck, J. G.; Seeberger, S.; Diederichs, K.; Moller, H. M.; Welte, W.; Wittmann, V. *J. Am. Chem. Soc.* **2010**, *132*, 8704.

(11) Munoz, E. M.; Correa, J.; Fernandez-Megia, E.; Riguera, R. *J. Am. Chem. Soc.* **2009**, *131*, 17765.

(12) (a) Mulder, A.; Auletta, T.; Sartori, A.; Del Ciotto, S.; Casnati, A.; Ungaro, R.; Huskens, J.; Reinhoudt, D. N. *J. Am. Chem. Soc.* **2004**, *126*, 6627. (b) Ercolani, G.; Piguet, C.; Borkovec, M.; Hamacek, J. *J. Phys. Chem. B* **2007**, *111*, 12195.

(13) Reynolds, M.; Pérez, S. *Comptes Rendus Chimie* **2011**, *14*, 74.

(14) (a) Fernandez-Megia, E.; Correa, J.; Rodríguez-Meizoso, I.; Riguera, R. *Macromolecules* **2006**, *39*, 2113. (b) Fernandez-Megia, E.; Correa, J.; Riguera, R. *Biomacromolecules* **2006**, *7*, 3104.

(15) For recent bioapplications of GATG dendrimers, see: (a) Raviña, M.; de la Fuente, M.; Correa, J.; Sousa-Herves, A.; Pinto, J.; Fernandez-Megia, E.; Riguera, R.; Sanchez, A.; Alonso, M. J. *Macromolecules* **2010**, *43*, 6953. (b) Fernández-Trillo, F.; Pacheco-Torres, J.; Correa, J.; Ballesteros, P.; Lopez-Larrubia, P.; Cerdán, S.; Riguera, R.; Fernandez-Megia, E. *Biomacromolecules* **2011**, *12*, 2902. (c) Albertazzi, L.; Fernandez-Villamarin, M.; Riguera, R.; Fernandez-Megia, E. *Bioconjugate Chem.* **2012**, *23*, 1059.

(16) Rich, R. L.; Myszka, D. G. *Curr. Opin. Biotechnol.* **2000**, *11*, 54.

(17) Lewis, S. D.; Shafer, J. A.; Goldstein, I. J. *Arch. Biochem. Biophys.* **1976**, *172*, 689.

(18) O'Shannessy, D. J.; Winzor, D. J. *Anal. Biochem.* **1996**, *236*, 275.

(19) (a) Williams, T. J.; Shafer, J. A.; Goldstein, I. J.; Adamson, T. *J. Biol. Chem.* **1978**, *253*, 8538. (b) Clegg, R. M.; Loontiens, F. G.; Van Landschoot, A.; Jovin, T. M. *Biochemistry* **1981**, *20*, 4687.

(20) Wolfenden, M. L.; Cloninger, M. J. *J. Am. Chem. Soc.* **2005**, *127*, 12168.

(21) For theoretical studies of rebinding phenomena, see: Lagerholm, B. C.; Thompson, N. L. *Biophys. J.* **1998**, *74*, 1215.

Table of Contents artwork